Supporting Information: On comparing packed beds and monoliths for CO_2 capture from air through experiments, theory and modeling

Valentina Stampi-Bombelli,[†] Alba Storione,[‡] Quirin Grossmann,[†] and Marco Mazzotti[*,†]

†Institute of Energy and Process Engineering, ETH Zurich, 8092 Zurich, Switzerland

‡Department of Civil, Chemical, Environmental and Materials Engineering (DICAM), Alma Mater Studiorum-University of Bologna, via Terracini 28, 40131 Bologna, Italy

E-mail: marco.mazzotti@ipe.mavt.ethz.ch

Phone: +41 44 632 24 56. Fax: +41 44 632 11 41

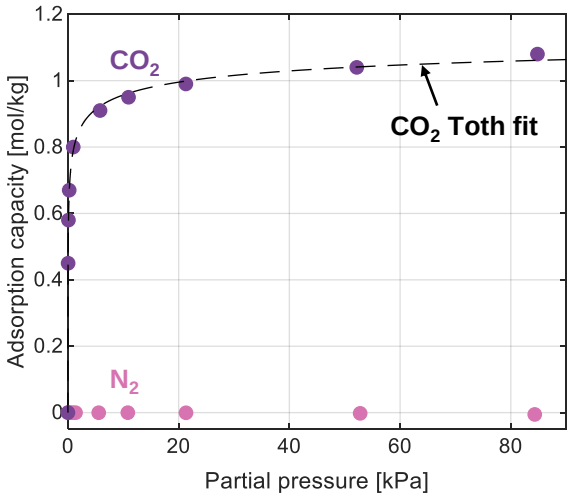

Figure S1: Pure N_2 (pink) and pure CO_2 (purple) equilibrium data at 298 K on the amine functionalized γ-alumina pellets presented in the work by Grossmann *et al.* and measured using a Microtrac Belsorp Max II volumetric device.[1] The black dashed line corresponds to the Toth fit of the CO_2 isotherm using the parameters presented in Table 1

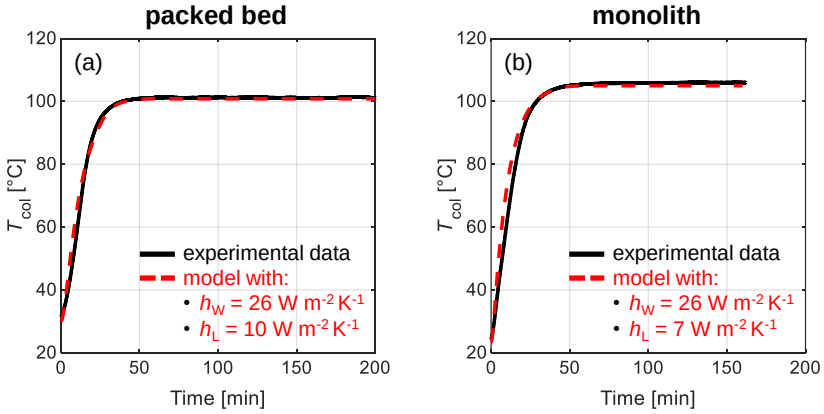

Figure S2: Temperature profiles experimentally measured in the packed bed column (at $z = 0.5L$) and in the monolith column (at $z = L$) in black, and the same temperatures predicted by the adsorption model in the dashed red curves

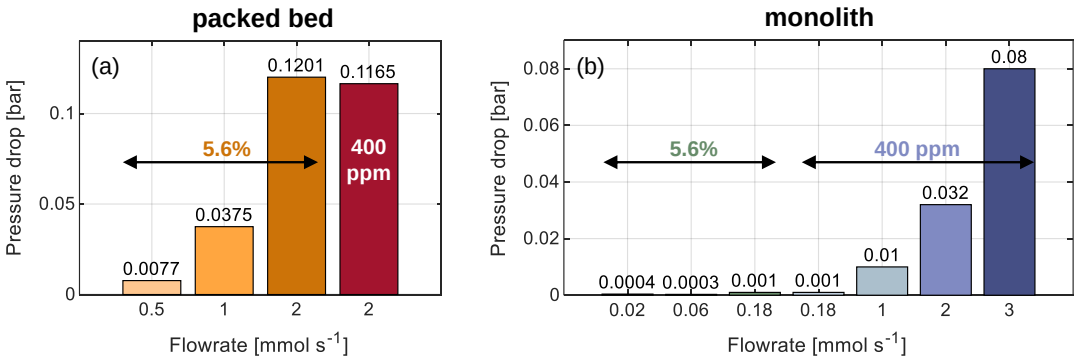

Figure S3: Experiment pressure drops of each conducted experiment, identified with the color and corresponding CO_2 mol fraction and total molar flow rate of the feed, measured across the (a) packed bed contactor; (b) monolith contactor

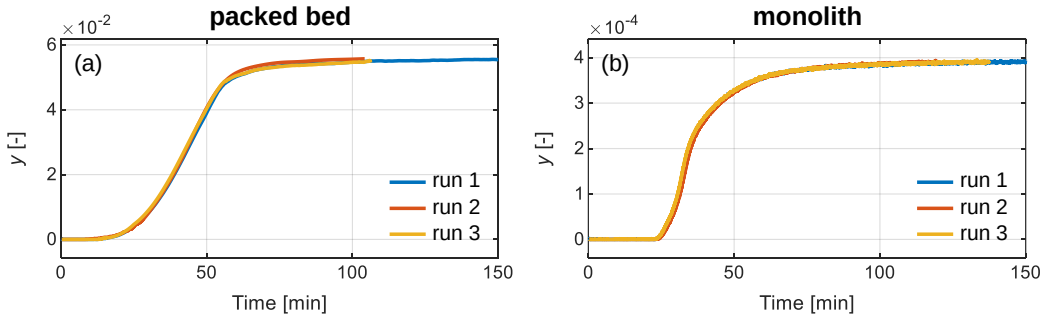

Figure S4: Reproducibility of the breakthrough experiments performed at 1 mmol s^{-1} on the (a) packed bed at 5.6%; (b) monolith at 400 ppm

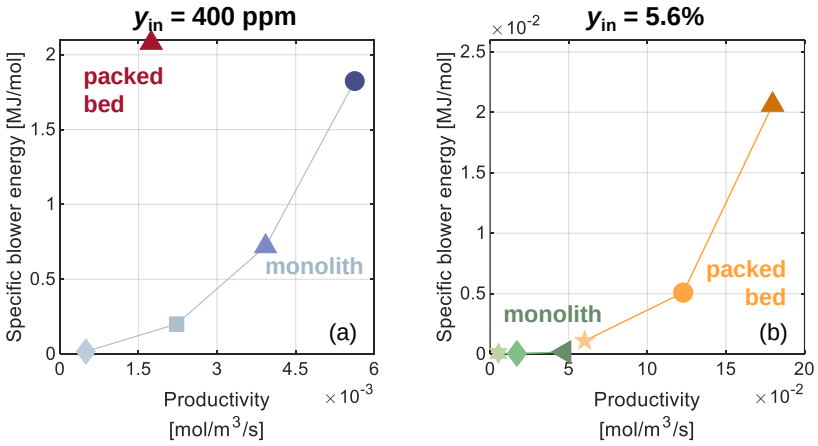

Figure S5: Specific energy demand plotted against the productivity of the adsorption step, expressed per volume of contactor, and comparison between the packed bed and monolith for all of the experiments performed in this study using a CO_2 inlet molar fraction of (a) y_{in} = 400 ppm, considering t_{90}; (b) y_{in} = 5.6%

S1 Constant pattern analysis

In the following, we present the derivation of the methodology proposed in Figure 3 for the identification of the major resistances governing adsorption using the constant pattern solution. In separation processes where kinetics dictate productivity, the ability to identify the limiting mechanisms that contribute to breakthrough profile dispersion is crucial for reducing resistances. While detailed rate-based models capture these resistances, such models can be numerically slow and complex. However, in adsorption systems, concentration profiles may attain a constant pattern behavior, exhibiting constant shape and velocity through the column. When a constant pattern exists, also known as a shock layer, the solution of the system can be greatly simplified and the system can be solved analytically through shock layer theory[2,3]. The following analysis aims at establishing a methodology based on the shock layer theory to elucidate such underlying mechanisms governing breakthrough profiles in adsorption systems. Our goal is to identify both axial dispersion and mass transfer resistances through experimental investigation of the mass transfer zones at different operating conditions, thereby establishing the methodology depicted in Figure 3. First, we outline the assumptions and equations necessary to computing the shock layer solution. Then, we evaluate the impact of varying feed operating conditions on the shock layer characteristics, which change based on which resistances are contributing the most to the shape of the breakthrough curve.

S1.1 Shock layer solution

A constant pattern, or shock layer, is assumed to exist on an infinitely long column, when the adsorption front reaches full development and thus remains unchanged. Adsorption systems characterized by favorable isotherms can often approximate this constant pattern behavior during adsorption even in columns of finite length. To compute the analytical solution of the shock layer, we adopt the approach introduced by Rhee and Amundson[2] and further extended by Mazzotti *et al.*[3]. Our primary objective is to demonstrate the practical applications of this analytical solution in the interpretation of breakthrough curves, thus we focus solely on introducing the pertinent equations

for this study. The analytical solution is derived from the gas and solid component mass balances under isothermal and isobaric conditions:

$$\psi\left(\frac{\partial c_i}{\partial \tau} + \nu^* \frac{\partial \hat{q}_i}{\partial \tau}\right) + \frac{\partial c_i}{\partial x} = \frac{1}{Pe_i}\frac{\partial^2 c_i}{\partial x^2} \tag{S1}$$

$$\frac{\partial \hat{q}_i}{\partial \tau} = St_i\left[\hat{q}_i^* - \hat{q}_i\right] \tag{S2}$$

where $\hat{q} = q\rho_s$ is the volume-based concentration in the solid crystals, $x = z/L$ and $\tau = ut/L$ are the dimensionless space and time coordinates and $St = kL/u$ and $Pe = uL/D_L$ are the dimensionless Stanton and Peclet numbers, respectively. For the constant pattern solution to exist, the following assumptions need to be fulfilled:

- The column is assumed to be infinitely long;
- The shock layer profile consists of a transition between the two states at the ends of the infinitely long column, where thermodynamic equilibrium is assumed. On the upstream far left, $c_L = c(-\infty, \tau)$ is the concentration of the inlet feed, at equilibrium with $\hat{q}_L = \hat{q}(-\infty, \tau) = \hat{q}^*(c_L)$. On the downstream far right, $c_R = c(+\infty, \tau)$ is the concentration of the adsorbate in the column prior to adsorption (initial state), at equilibrium with $\hat{q}_R = \hat{q}(+\infty, \tau) = \hat{q}^*(c_R)$;
- The shock layer, which is the transition from c_L to c_R, travels at a constant dimensionless velocity λ, such that the speed of propagation is defined by $\tilde{u} = u\lambda$.

It follows that the constant pattern solution can be expressed with a single moving coordinate defined as: $\xi = x - \lambda\tau$. For an analytical expression of the shock layer profile to exist, a further assumption needs to be fulfilled:

- The product of *Pe* and *St* needs to be much larger than 1, such that the second order term of Equation (21) in the work presented by Mazzotti *et al.* is negligible with respect to the other terms.[3]

In the derivation of the constant pattern solution, we consider a system subjected to the single-component Langmuir isotherm:

$$\hat{q}_i^*(c_i) = \frac{nKc_i}{1 + Kc_i} \tag{S3}$$

To be consistent with the multicomponent analysis presented by Mazzotti *et al.*, we define the variable δ, as:

$$\delta = 1 + Kc \tag{S4}$$

If the assumptions presented above are fulfilled, the analytical expression for ξ as a function of δ can be computed, that fulfills the conditions $\delta_L = \delta(-\infty) > \delta > \delta_R = \delta(+\infty)$:

$$\xi = \frac{1}{\alpha\vartheta}\frac{1}{\delta_L - \delta_R}\left(\delta_L \ln\frac{\delta_L - \delta}{\delta_L - \delta_0} - \delta_R \ln\frac{\delta - \delta_R}{\delta_0 - \delta_R}\right) \tag{S5}$$

where α is a parameter containing information on the axial dispersion and mass transfer resistances, ϑ contains information on the equilibrium states at the column ends, and δ_0 is the inflection point of the shock layer (as respectively defined by Equations (37), (100) and (83) in the work by Mazzotti *et al.*):[3]

$$\frac{1}{\alpha} = \frac{1}{\psi\nu^*}\left(\frac{1}{\lambda Pe} + \frac{1 - \psi\lambda}{St}\right) \tag{S6}$$

$$\vartheta = \frac{\hat{q}_L - \hat{q}_R}{c_L - c_R} \tag{S7}$$

$$\delta_R \ln(\delta_0 - \delta_R) - \delta_L \ln(\delta_L - \delta_0) = (\delta_L - \delta_R)[1 - \ln(\delta_R - \delta_L)] \tag{S8}$$

$$\lambda = \frac{1}{\psi(1 + \nu^*\vartheta)} \quad \text{and} \quad \frac{1 - \psi\lambda}{\lambda} = \nu^*\psi\vartheta \tag{S9}$$

The shock layer profile from state δ_L to δ_R as a function of the moving coordinate ξ is described by Equation (S5). The concentration profile in the column can be determined by computing c against x at any specified time τ. Moreover, the breakthrough profiles can be readily determined by computing c against time (τ) at the column outlet, where $x = 1$.

S1.2 Computing the shock layer thickness

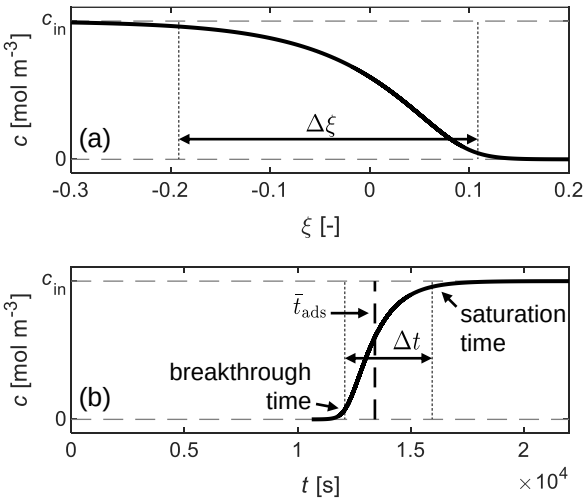

Figure S6: Adsorption profile using a feed with concentration and velocity of $c_{\text{in}} = 0.04\ \text{mol}\,\text{m}^{-3}$ and $u = 0.036\ \text{m}\,\text{s}^{-1}$, respectively (with $\lambda = 0.0003$, $\vartheta = 1648$, $\nu^* = 0.22$, $\psi = 2.15$), computed using the constant pattern solution and plotted against: (a) the moving coordinate, ξ; (b) time, t, at the column exit

An example of a concentration shock layer plotted against ξ, as derived from Equation (S5), is presented in Figure S6a, alongside the associated breakthrough profile at the column exit, shown in Figure S6b. The shock layer thickness, $\Delta\xi$, is observed in relation to the mass transfer zone thickness, Δt. When equilibrium and transport properties are well-defined, determining the shock layer thickness becomes straightforward as its calculation becomes independent of δ_0, thereby eliminating the need to solve Equation (S5). To this end, we introduce two concentration bounds, δ_* and δ^*, equidistant from the extreme values δ_L and δ_R at a relative distance β:

$$\beta = \frac{\delta_L - \delta^*}{\delta_L - \delta_R} = \frac{\delta_* - \delta_R}{\delta_L - \delta_R} \tag{S10}$$

The shock layer thickness between these two bounds is defined as $\Delta\xi = \xi(\delta_*) - \xi(\delta^*)$, and utilizing Equation (S5), it can be expressed as:

$$\Delta\xi = \frac{1}{\alpha\vartheta}\frac{\delta_L + \delta_R}{\delta_L - \delta_R}\ln\left(\frac{1-\beta}{\beta}\right) \tag{S11}$$

The relationship between the mass transfer zone thickness, Δt, and the shock layer thickness, $\Delta\xi$ is established by evaluating the shock layer thickness at the column exit:

$$\Delta\xi = \xi_1 - \xi_2 = 1 - \lambda\tau_1 - 1 + \lambda\tau_2 \tag{S12}$$

$$= \lambda\Delta\tau = \frac{\Delta\tau}{\bar{\tau}_{\text{ads}}} \tag{S13}$$

$$= \frac{\Delta t}{\bar{t}_{\text{ads}}} \tag{S14}$$

where $\bar{t}_{\text{ads}}$ represents the mean residence time, an intrinsic property determined by the column size, feed flow rate, and feed concentration, defined as:

$$\bar{t}_{\text{ads}} = \frac{L}{u}\frac{\varepsilon^*}{\varepsilon}\left(1 + \frac{1-\varepsilon^*}{\varepsilon^*}\frac{\hat{q}^*_{\text{in}}}{c_{\text{in}}}\right) = \frac{L}{u}\frac{1}{\lambda} \tag{S15}$$

$$\bar{\tau}_{\text{ads}} = \frac{1}{\lambda} \tag{S16}$$

In practical applications, the mean residence time is often approximated using the 50% breakthrough time (t_{50}), which is the time at which the concentration reaches half of the inlet concentration, $c = 0.5c_{\text{in}}$.

S1.3 Identifying the limiting dispersion mechanisms

In most separations, dispersion phenomena due to mass transfer resistances and axial dispersion contribute to broadening the shock layer thickness ($\Delta\xi$) and mass transfer zone thicknesses (Δt and $\Delta\tau$). Our objective in this section is to use the definition of shock layer thickness, as presented in Equation (S11), to discern whether axial dispersion or mass transfer resistances are the predominant factors shaping the breakthrough profile. We illustrate how changes in velocity and feed concentration distinctly affect $\Delta\xi$, Δt, and $\Delta\tau$, depending on the prevailing dominant mechanism. For the purpose of this analysis, we define that column is completely regenerated at the beginning

of adsorption, thus:

$$\frac{\delta_L + \delta_R}{\delta_L - \delta_R} = \frac{2 + Kc_{\text{in}}}{Kc_{\text{in}}} = \Gamma \tag{S17}$$

$$\vartheta = \hat{q}_{\text{in}}/c_{\text{in}} \tag{S18}$$

S1.3.1 Effect of feed velocity

When maintaining constant feed concentration, a change in feed velocity solely affects α, while all the other terms remain constant; then, the reformulated equation for $\Delta\xi$ is as follows:

$$\Delta\xi(u) = C_1 \frac{1}{\alpha} \text{ with } C_1 = \frac{1}{\vartheta}\Gamma \ln\left(\frac{1-\beta}{\beta}\right) = \text{constant} \tag{S19}$$

$$= C_1 \nu^* \psi \left[\frac{1}{\lambda Pe(u)} + \frac{1-\psi\lambda}{St(u)}\right] \tag{S20}$$

$$= C_1 \nu^* \psi \left[\frac{D_L}{\lambda L}\frac{1}{u} + \frac{1-\psi\lambda}{k(u)L}u\right] \tag{S21}$$

The variation of $\Delta\xi$ with an increase in velocity, u, depends on whether axial dispersion or mass transfer resistances govern adsorption. To assess this, we compute the derivative of $\Delta\xi$ with respect to u. Within the axial dispersion term of Equation (S21), velocity appears in the denominator, while in the mass transfer resistance term, it appears in the numerator. Thus, when axial dispersion is the primary mechanism, the Peclet term predominates and the derivative in u is negative, causing $\Delta\xi$ to decrease with an increase in velocity. On the contrary, as the variation of mass transfer coefficients with velocity is typically negligible, when mass transfer resistances are the primary mechanism, the Stanton term predominates and the derivative in u is positive, leading to an increase in $\Delta\xi$ with rising velocity. This same pattern applies to changes $\Delta\tau = \Delta\xi/\lambda$ with velocity, but it does not hold true for $\Delta t = (\Delta\xi L)/(\lambda u)$ due to the different contribution of velocity.

Limiting cases: only one mechanism governing adsorption

Variations in feed velocity provide insights into the primary mechanism influencing adsorption,

observable through changes in $\Delta\xi$ and $\Delta\tau$. Limiting cases where a single mechanism entirely dictates the breakthrough profile's shape can exist, and computing the ratio of $\Delta\tau$ at different velocities becomes a valuable strategy to assess these cases. Given that all terms except $1/\alpha$ remain constant during velocity change, the ratio of $\Delta\tau$ from u_1 to u_2 is formulated as:

$$\frac{\Delta\tau_{u_1}}{\Delta\tau_{u_2}} = \frac{\alpha_2}{\alpha_1} = \frac{\left(\frac{1}{\lambda Pe_1} + \frac{1-\psi\lambda}{St_1}\right)}{\left(\frac{1}{\lambda Pe_2} + \frac{1-\psi\lambda}{St_2}\right)} \tag{S22}$$

In cases where adsorption is solely governed by either mass transfer or axial dispersion, simplification of the ratio becomes possible by eliminating one of the two dimensionless numbers from both the numerator and denominator. In Table S1, we explore the various scenarios that can arise when specific contributions entirely govern adsorption. Interestingly, these limiting scenarios can be experimentally identified when the ratio of $\Delta\tau$ at two distinct velocities simplifies to either unity or a known ratio of the two velocities, bypassing the need for exact k or D_L values. Figure 3 elaborates on the experimental approach for discerning the roles of axial dispersion and mass transfer resistances by manipulating feed velocity.

S1.3.2 Effect of feed concentration

While altering feed velocity is insightful for discerning whether axial dispersion or mass transfer resistances are the limiting factors in adsorption, it falls short in differentiating among various mass transfer resistances. These resistances could be those in the gas film, in the pores of the particle, or in the solid phase, as indicated by the different mass transfer contributions in Equation 6. To make this distinction, it is necessary to investigate the effect of changing the feed concentration on the breakthrough profile. Changing the feed concentration has an impact on several terms in the shock layer thickness equation, specifically $1/\alpha$, $1/\vartheta$, and Γ, and can lead to changes in $\Delta\xi$ stemming from any of these terms. Consequently, identifying axial dispersion and mass transfer resistances within α can pose a challenge. While the variation of $1/\vartheta$ with c_{in} remains essential in

our analysis, under certain circumstances, neglecting the effect of Γ as the concentration varies can be justified. This is because chemisorbents are often chosen for low-concentration gas separations (c small, K large) and physisorbents are suitable for high-concentration gas separations (c large, K small), thus yielding a constant Γ with c_{in}. In this study, we focus on steep isotherms with large K values and omit the consideration of Γ. As a result, for an adsorbent with a steep isotherm, $\Delta\xi$ simplifies to Equation (S23), with concentration dependence only in α and ϑ. Considering that λ is typically very small, the terms $1 - \psi\lambda \approx 1$ and $\lambda\vartheta \approx 1/(\nu^*\psi)$ are constant, leading us to the final form of $\Delta\xi$ in Equation (S25):

$$\Delta\xi(c_{\text{in}}) = C_2 \frac{1}{\alpha\vartheta} \text{ with } C_2 = \Gamma \ln\left(\frac{1-\beta}{\beta}\right) = \text{constant} \tag{S23}$$

$$= C_2 \left[\frac{1}{\lambda\vartheta Pe} + \frac{1-\lambda\psi}{St\vartheta}\right] \tag{S24}$$

$$\approx C_2 \left[\frac{\nu^*\psi}{Pe} + \frac{\rho_p}{\rho_s}\frac{u}{L}\left(\frac{1}{k_f} + \frac{1}{k_p}\right) + \lambda(c_{\text{in}})\frac{u}{L}\frac{1}{k_s}\right] \tag{S25}$$

The expression for $\Delta\xi$ consists of three terms: axial dispersion, mass transfer resistance in the gas phases (gas film and sorbent pores), and mass transfer resistance in the solid phase. Among these terms, only the mass transfer resistance within the solid phase, through parameter λ, exhibits concentration dependence. The positive derivative of λ with respect to c implies that $\Delta\xi$ increases with an increase in feed concentration. In contrast, the derivative of $\Delta\xi$ in c in the two terms associated with gas-phase resistances, whether related to axial dispersion or mass transport in the gas, yields zero. Consequently, when gas-phase resistances dominate, $\Delta\xi$ remains constant with variations in feed concentration.

Limiting cases: only one mechanism governing adsorption

In situations where a single resistance significantly prevails, evaluating the ratio of $\Delta\xi$ for different feed concentrations can offer valuable insights, similar to the approach taken for the $\Delta\tau$ ratio in velocity variation:

$$\frac{\Delta\xi_{c_1}}{\Delta\xi_{c_2}} = \frac{\alpha_2}{\alpha_1}\frac{\vartheta_2}{\vartheta_1} = \frac{\vartheta_2}{\vartheta_1}\frac{\left[\dfrac{1}{\lambda_1 Pe} + \dfrac{1-\psi\lambda_1}{St_1}\right]}{\left[\dfrac{1}{\lambda_2 Pe} + \dfrac{1-\psi\lambda_2}{St_2}\right]} \tag{S26}$$

Similar to the velocity analysis, when axial dispersion or mass transfer mechanisms entirely dominate the process, either Stanton or Peclet can be simplified from the numerator and the denominator. In the case of mass transfer control, further simplifications are made given the different dependencies on concentration in the various terms of the overall mass transfer coefficient, as previously highlighted in Equation (S25). In Table S2, we explore the limiting scenarios and the simplified ratios that derive thereof, allowing the differentiation of gas-phase and solid-phase resistances with no prior knowledge on k_f, k_p and k_s. In Step 2 of Figure 3, we summarize the proposed general approach to distinguish the dissipation mechanisms through the variation in feed concentration.

Table S1: Effect of changing the feed velocity at constant concentration (λ and ϑ constant) on the ratios of Δt and $\Delta\tau$. General case and extreme cases with a unique rate-limiting dispersion mechanism

General case

$$\frac{\Delta t_1}{\Delta t_2} = \frac{u_2}{u_1}\frac{\alpha_2}{\alpha_1} = \frac{u_2}{u_1}\frac{\left(\frac{1}{\lambda Pe_1} + \frac{1-\psi\lambda}{St_1}\right)}{\left(\frac{1}{\lambda Pe_2} + \frac{1-\psi\lambda}{St_2}\right)} \quad \text{(S27)} \qquad \frac{\Delta\tau_1}{\Delta\tau_2} = \frac{\alpha_2}{\alpha_1} = \frac{\left(\frac{1}{\lambda Pe_1} + \frac{1-\psi\lambda}{St_1}\right)}{\left(\frac{1}{\lambda Pe_2} + \frac{1-\psi\lambda}{St_2}\right)} \quad \text{(S28)}$$

Extreme cases

A. *Pe* limiting: $\lambda Pe \ll (1-\psi\lambda)St$

$$\frac{\Delta t_1}{\Delta t_2} = \frac{u_2}{u_1}\frac{Pe_2}{Pe_1} = \frac{u_2^2}{u_1^2}\frac{D_{L,1}}{D_{L,2}} \quad \text{(S29)} \qquad \frac{\Delta\tau_1}{\Delta\tau_2} = \frac{Pe_2}{Pe_1} = \frac{u_2}{u_1}\frac{D_{L,1}}{D_{L,2}} \geq 1 \quad \text{(S30)}$$

A1. Constant axial dispersion coefficient: $D_{L,1} = D_{L,2}$

$$\frac{\Delta t_1}{\Delta t_2} = \frac{u_2^2}{u_1^2} \quad \text{(S31)} \qquad \frac{\Delta\tau_1}{\Delta\tau_2} = \frac{u_2}{u_1} \quad \text{(S32)}$$

A2. Peclet constant: $Pe_1 = Pe_2$

$$\frac{\Delta t_1}{\Delta t_2} = \frac{u_2}{u_1} \quad \text{(S33)} \qquad \frac{\Delta\tau_1}{\Delta\tau_2} = 1 \quad \text{(S34)}$$

B. *St* limiting: $(1-\psi\lambda)St \ll \lambda Pe$

$$\frac{\Delta t_1}{\Delta t_2} = \frac{u_2}{u_1}\frac{St_2}{St_1} = \frac{k_2}{k_1} \quad \text{(S35)} \qquad \frac{\Delta\tau_1}{\Delta\tau_2} = \frac{St_2}{St_1} = \frac{k_2}{k_1}\frac{u_1}{u_2} < 1 \quad \text{(S36)}$$

B1. Rate-limiting step in fluid film: $k = k_f(u)$

$$\frac{\Delta t_1}{\Delta t_2} = \frac{k_{f,2}}{k_{f,1}} \quad \text{(S37)} \qquad \frac{\Delta\tau_1}{\Delta\tau_2} = \frac{k_{f,2}}{k_{f,1}}\frac{u_1}{u_2} \quad \text{(S38)}$$

B2. Rate-limiting step in fluid pore or in solid: $k_1 = k_2$

$$\frac{\Delta t_1}{\Delta t_2} = 1 \quad \text{(S39)} \qquad \frac{\Delta\tau_1}{\Delta\tau_2} = \frac{u_1}{u_2} \quad \text{(S40)}$$

Table S2: Effect of changing the feed concentration at constant velocity (u and Pe constant) for a sorbent with steep isotherms, i.e. $K \gg 1$ such that $\lambda_i \vartheta_i \approx$ constant; $1 - \psi\lambda \approx 1$; $\lambda_2/\lambda_1 \approx \vartheta_1/\vartheta_2 \approx c_2/c_1$

General case, $K \gg 1$

$$\frac{\Delta t_1}{\Delta t_2} = \frac{\alpha_2}{\alpha_1} = \frac{\left(\frac{1}{\lambda_1 Pe} + \frac{1-\psi\lambda_1}{St_1}\right)}{\left(\frac{1}{\lambda_2 Pe} + \frac{1-\psi\lambda_2}{St_2}\right)} \quad \text{(S41)} \qquad \frac{\Delta\xi_1}{\Delta\xi_2} = \frac{\alpha_2}{\alpha_1}\frac{\vartheta_2}{\vartheta_1} = \frac{\vartheta_2}{\vartheta_1}\frac{\left(\frac{1}{\lambda_1 Pe} + \frac{1-\psi\lambda_1}{St_1}\right)}{\left(\frac{1}{\lambda_2 Pe} + \frac{1-\psi\lambda_2}{St_2}\right)} \quad \text{(S42)}$$

Extreme cases, $K \gg 1$

A. *Pe* limiting: $\lambda Pe \ll (1-\psi\lambda)St$

$$\frac{\Delta t_1}{\Delta t_2} = \frac{\lambda_2}{\lambda_1} \approx \frac{c_2}{c_1} \quad \text{(S43)} \qquad \frac{\Delta\xi_1}{\Delta\xi_2} = \frac{\lambda_2\vartheta_2}{\lambda_1\vartheta_1} \approx 1 \quad \text{(S44)}$$

B. *St* limiting: $(1-\psi\lambda)St \ll \lambda Pe$

$$\frac{\Delta t_1}{\Delta t_2} \approx \frac{St_2}{St_1} = \frac{k_2}{k_1} \quad \text{(S45)} \qquad \frac{\Delta\xi_1}{\Delta\xi_2} = \frac{\lambda_1}{\lambda_2}\frac{St_2}{St_1} = \frac{\lambda_1}{\lambda_2}\frac{k_2}{k_1} \quad \text{(S46)}$$

B1. Rate-limiting step in fluid (film and/or pore): $k_2/k_1 = \vartheta_1/\vartheta_2$

$$\frac{\Delta t_1}{\Delta t_2} = \frac{c_2/q_2}{c_1/q_1} \approx \frac{c_2}{c_1} \quad \text{(S47)} \qquad \frac{\Delta\xi_1}{\Delta\xi_2} = \frac{\lambda_1\vartheta_1}{\lambda_2\vartheta_2} \approx 1 \quad \text{(S48)}$$

B2. Rate-limiting step in solid: $k_1 = k_2 = k_s$

$$\frac{\Delta t_1}{\Delta t_2} = 1 \quad \text{(S49)} \qquad \frac{\Delta\xi_1}{\Delta\xi_2} = \frac{\lambda_1}{\lambda_2} \approx \frac{c_1}{c_2} \quad \text{(S50)}$$

References

(1) Grossmann, Q.; Stampi-Bombelli, V.; Yakimov, A.; Docherty, S.; Copéret, C.; Mazzotti, M. Developing Versatile Contactors for Direct Air Capture of CO2 through Amine Grafting onto Alumina Pellets and Alumina Wash-Coated Monoliths. *Ind. Eng. Chem. Res.* **2023**, *62*, 13594–13611.

(2) Rhee, H. k.; Amundson, N. R. Shock layer in two solute chromatography: effect of axial dispersion and mass transfer. *Chem. Eng. Sci.* **1974**, *29*, 2049–2060.

(3) Mazzotti, M.; Storti, G.; Morbidelli, M. Shock layer analysis in multicomponent chromatography and countercurrent adsorption. *Chem. Eng. Sci.* **1994**, *49*, 1337–1355.

(4) Patton, A.; Crittenden, B. D.; Perera, S. P. Use of the linear driving force approximation to guide the design of monolithic adsorbents. *Chem. Eng. Res. Des.* **2004**, *82*, 999–1009.

Notation

Roman symbols

A	column cross section	$[\mathrm{m}^2]$
c	gas phase concentration	$[\mathrm{mol\,m}^{-3}]$
d_p	pellet diameter	[m]
d_{pore}	diameter of the γ-alumina pore	[m]
D	column diameter	[m]
D_{al}	effective diffusivity in the γ-alumina pockets	$[\mathrm{m}^2\,\mathrm{s}^{-1}]$
D_p	effective diffusivity in the pellet pore	$[\mathrm{m}^2\,\mathrm{s}^{-1}]$
D_m	molecular diffusion	$[\mathrm{m}^2\,\mathrm{s}^{-1}]$
D_{mullite}	effective diffusivity in the mullite pores	$[\mathrm{m}^2\,\mathrm{s}^{-1}]$
D_s	crystalline diffusivity	$[\mathrm{m}^2\,\mathrm{s}^{-1}]$
D_L	axial dispersion coefficient	$[\mathrm{m}^2\,\mathrm{s}^{-1}]$
k	LDF overall mass transfer coefficient	$[\mathrm{s}^{-1}]$
K	Langmuir equilibrium constant	$[\mathrm{m}^3\,\mathrm{mol}^{-1}]$
k_f	film mass transfer coefficient	$[\mathrm{s}^{-1}]$
k'_f	film mass transfer coefficient	$[\mathrm{m\,s}^{-1}]$
k_p	pore mass transfer coefficient	$[\mathrm{s}^{-1}]$
$k_{p,\mathrm{al}}$	mass transfer coefficient in the γ-alumina pocket mesopores	$[\mathrm{s}^{-1}]$
$k_{p,\mathrm{mullite}}$	mass transfer coefficient in the mullite macropores	$[\mathrm{s}^{-1}]$
k_s	solid mass transfer coefficient	$[\mathrm{s}^{-1}]$

L	column length	[m]
M	molecular weight	[g mol^{-1}]
m_s	sorbent mass	[kg]
$\dot{n}$	molar flow rate	[mol s^{-1}]
N	total number of cells in the monolith	[-]
p	pressure	[Pa]
Pe	Peclet number, [$= uL/D_L$]	[-]
q	mass-based adsorbed-phase concentration	[mol kg$^{-1}{}_{\text{sorbent}}$]
q_p	volume-based adsorbed-phase concentration, [$= q\rho_{\text{p}}$]	[mol m^{-3}]
$\hat{q}$	volume-based adsorbed-phase concentration, [$= q\rho_{\text{s}}$]	[mol m^{-3}]
q^*	solid loading at equilibrium with c	[mol kg^{-1}]
r_1	internal hydraulic diameter of the square monolith channel,[4] [$= 2w_1/\pi$]	[m]
r_2	external hydraulic diameter of the square monolith channel,[4] [$= \left(4w_{wall}w_2/pi + r_1^2\right)^{0.5}$]	[m]
r_{al}	radius of γ-alumina pockets	[m]
r_c	crystalline radius	[m]
r_p	pellet radius	[m]
Re	Reynolds number, [$= \rho u_s d_p/\mu$]	[-]
Sc	Schmidt number, [$= \mu/(\rho D_m)$]	[-]
Sh	Sherwood number	[-]
St	Stanton number, [$= kL/u$]	[-]

t	time	[s]
T	temperature	[K]
u	interstitial velocity, [$= u_s/\varepsilon$]	[$\mathrm{m\,s^{-1}}$]
u_s	superficial velocity	[$\mathrm{m\,s^{-1}}$]
$\dot{V}$	volumetric flow rate of the gas feed	[$\mathrm{m^3\,s^{-1}}$]
W	monolith width	[m]
w_1	monolith void channel width	[m]
w_2	monolith cell width, [$w_2 = w_1 + w_{wall}$]	[m]
W_{fan}	specific blower energy consumption	[$\mathrm{MJ\,mol^{-1}}$]
w_{wall}	monolith wall thickness	[m]
x	dimensionless axial coordinate, [$= z/L$]	[-]
y	CO_2 molar fraction	[-]
z	axial coordinate	[m]

Greek Symbols

α	parameter of the shock layer	[-]
β	percentage of the feed concentration in the shock layer analysis	[-]
Δp	pressure drop across the column	[Pa]
ε	bed void fraction	[-]
$\varepsilon_{\mathrm{al}}$	void fraction of the γ-alumina pockets in the monolith	[-]

ε_p	pellet/wall void fraction	[-]
ε^*	total void fraction, [$= \varepsilon + \varepsilon_p(1-\varepsilon)$]	[-]
Γ	parameter of the shock layer	[-]
λ	dimensionless shock velocity	[-]
μ	dynamic viscosity	[Pa s]
ν	capacity ratio, [$= (1-\varepsilon)/\varepsilon$]	[-]
ν^*	capacity ratio, [$= (1-\varepsilon^*)/\varepsilon^*$]	[-]
ξ	moving coordinate, [$= z - \lambda\tau$]	[-]
ψ	porosity ratio, [$= \varepsilon^*/\varepsilon$]	[-]
ρ_b	bed density	[kg m$^{-3}_{\text{COLUMN}}$]
ρ_p	pellet density	[kg m$^{-3}_{\text{PELLET}}$]
ρ_s	solid density	[kg m$^{-3}_{\text{SOLID}}$]
τ	dimensionless time, [$= tu/L$]	[-]
τ_{al}	γ-alumina tortuosity	[-]
$\tau_{mullite}$	mullite tortuosity	[-]
ϑ	parameter of the shock layer	[-]

Subscripts and Superscripts

in	feed conditions

Acronyms

CPSI	Cells per square inch
DAC	Direct air capture
KPI	Key performance indicator
LDF	Linear driving force
MFC	Mass flow controler
MTZ	Mass transfer zone
NET	Negative emission technologies